V International Conference on Computational Methods in Marine Engineering
MARINE 2013
B. Brinkmann and P. Wriggers (Eds)

EFFECT OF THE BENDING STIFFNESS ON THE VOLUMETRIC STABILITY OF FISH CAGES WITH COPPER ALLOY NETTING

JUDSON C. DECEW[*], MICHAEL OSIENSKI[*], ANDREW DRACH[†], BARBAROS CELIKKOL[†], IGOR TSUKROV[†]

[*] Center for Ocean Engineering
University of New Hampshire
Durham, NH 03824, USA
e-mail: jud.decew@unh.edu

[†] Department of Mechanical Engineering
University of New Hampshire
Durham, NH 03824, USA
e-mail: igor.tsukrov@unh.edu

Key words: Aquaculture, Volumetric Stability, Numerical Modeling

Abstract. It has been well established that aquaculture will supply an increasing share of the world's seafood demand in the future. Most finfish are raised in marine fish cages consisting of a floating superstructure, polymer net chamber and a sinker weight(s). These systems are susceptible to large deformations, which can lead to reduction of the cage's volume and severely impact the health of the fish stock.

Net chamber deformation could be mitigated with the use of stiffer netting, such as copper alloy mesh. However, little is known regarding the bending characteristics of copper alloy nets and their relationship to the volumetric deformation of a fish cage. In this study, numerical modeling tools and techniques are developed and used to predict the dynamic structural behavior of gravity fish cages with copper alloy. An analytical model is validated by experimental testing to obtain an equivalent flexural rigidity. The model is used for finite element studies of the effect of bending resistance on the volume loss of fish cages with copper alloy netting. The contribution of the copper alloy's bending resistance to the volumetric stability is found to be minimal for the tested configurations. Thus, the traditional numerical modeling techniques (i.e. using truss elements) are sufficient for analyzing copper alloy cage configurations.

1. INTRODUCTION

The growth of global population, presently at 7 billion and projected to reach 9.3 billion in 2050, will continue to pressure the worldwide food supply [1]. Presently, 16% of the globally consumed animal protein comes from capture fisheries and aquaculture. With the wild fish stock population plateauing due to overfishing, aquaculture is expected to increase its seafood contributions by 8% a year for the foreseeable future [2].

The most commonly utilized containment system used by the marine aquaculture industry is called a gravity type cage. This type of cage system traditionally consists of a buoyant collar

made of high density polyethylene (HDPE), a polymer (nylon) net chamber suspended below the buoyant collar, and a weighted lower collar. The lower collar is typically filled with steel chain or other similar dense materials to keep the net vertical and resist deformation. This type of cage system relies on the difference in forces between the weighted net chamber and the main floatation collar to act as the restorative force which sustains the volume of a net chamber. In this configuration, fish cages are susceptible to net chamber deformation caused by substantial lateral forces or by inertial movements of components, which can decrease the net chamber volume. Significant reduction of the net chamber volume has been documented to occur when the system is subjected to high energy conditions (see for example [3, 4, 5]) and/or marine biological growth on the net chamber [6, 7]. An excessive chamber volume loss can lead to short-term crowding of the fish population, resulting in a hormonal stress response and reduced growth rates [8].

Copper alloy nets have been presented as a solution to fish cage volume loss due their inherent fouling resistance [9], high strength [10], and prevention of predation common in polymer nets [11]. However, most of the copper alloy research has focused on its fouling resistance, material loss rates [12], or the hydrodynamic characteristics of the netting [9, 13] and not on the effect of mesh bending stiffness on fish cage volumetric stability. In this study, the effective area moment of inertia of three copper alloys were found and used to investigate the effectiveness of this material to resist net chamber deformation using a combination of analytical models, finite element simulations, and laboratory experiments.

2. DESCRIPTION OF THE INVESTIGATED COPPER ALLOY MESHES

The most widely used copper alloy net in aquaculture cages is of the “chain-link” type. This net type (Figure 1) is typically hung with pickets in the vertical (warp) direction. In this orientation, wires (called pickets) are structurally independent of its interconnected/linked neighbors. Thus, if any single picket fails, the structural integrity of the net chamber is maintained. If the pickets were oriented in the horizontal direction, the failure of a single picket would lead to an expanding hole opened by the gravity forces. In the vertical orientation, the pickets provide certain bending resistance which could reduce the net chamber deformations. Note that the resistance to bending is only present when the mesh is loaded in the warp direction; in the weft direction, the pickets are effectively unrestricted.

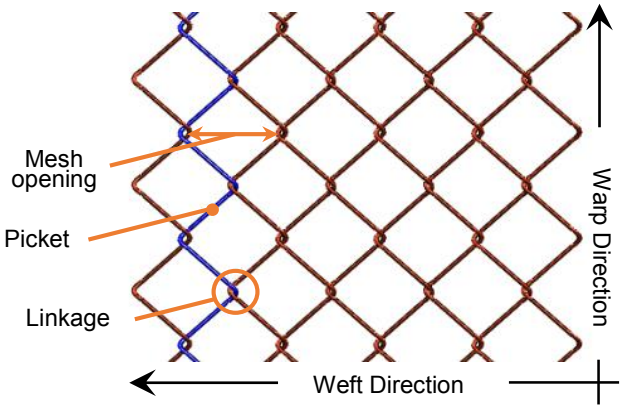

Figure 1: Chain-link mesh diagram.

Table 1: Material properties of the copper-alloy meshes.

Mesh parameters	Mesh type		
Mesh denomination	M2.5-25	M3.5-50	M2.5-30
Alloy name	Admiralty Brass, UR30	Silicon Bronze, SeaWire	Admiralty Brass, BlueSteel
Mesh opening, *mm*	25	50	30
Wire diameter, *mm*	2.5	3.5	2.5
Young's modulus, GPa	102	113	109
Shear modulus, GPa	38	42	41
Poisson's ratio	0.35	0.36	0.32
Density, kg/m^3	8300	8400	8400

Three of the most commonly utilized copper alloy mesh types were chosen for analysis. All three are of "chain-link" configuration: *M2.5-25* manufactured by Mitsubishi Shindoh; *M2.5-30* manufactured by Wieland-Werke; and *M3.5-50* manufactured by Luvata Appleton. Their material and geometric properties are shown in Table 1. Note that the denominations *M2.5-25*, *M2.5-30*, and *M3.5-50* are based on the wire diameter and the mesh opening size of the meshes.

3. ANALYTICAL METHOD FOR DETERMINING AREA MOMENT OF INERTIA

The first step is to construct an analytical model to describe the bending resistance, or more importantly, the equivalent area moment of inertia of pickets for each mesh. Due to the complex three dimensional geometry of the mesh, an average value for the area moment of inertia over the picket length is obtained. For this, each picket is assumed to act independently from the mesh as a whole. Only one repetitious segment of a picket can be considered due to the periodicity of its geometry, see Figure 2a.

Analytical modeling is based on the analysis of the picket's internal strain energy due to deformation. This energy can be represented as a sum of bending, shear, torsion, and axial components. To obtain the total strain energy of the system, an imaginary force F is applied to one end of the half segment, with the other end assumed to be rigidly fixed. For this type of loading, the contribution of axial and shear terms is much smaller than that of bending and torque. Thus, the strain energy is

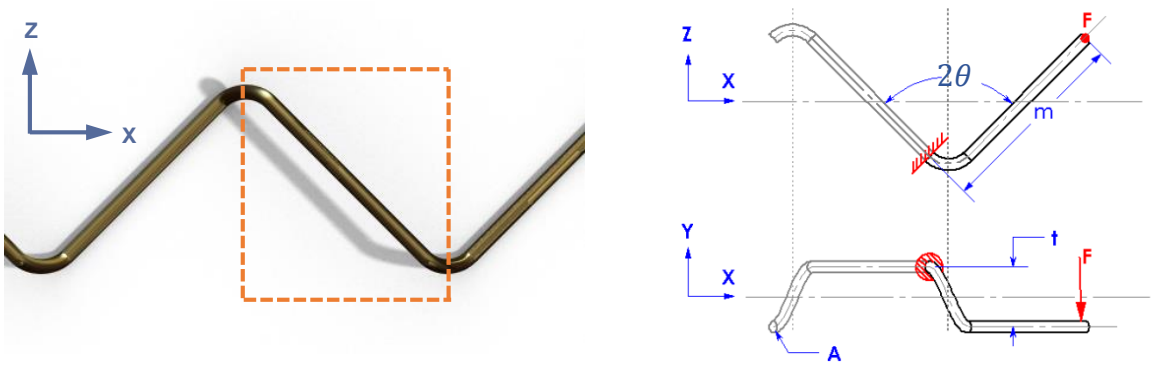

Figure 2: Chain-link picket geometry: (a) repetitious segment; (b) force diagram.

$$U_{Total} = \int_0^L \frac{M^2(x)}{2EI_{zz}} dx + \int_0^L \frac{T^2(x)}{2GJ_0} dx \tag{1}$$

where x is the distance along the warp direction; L is the total length of the picket segment along the warp direction; M is the bending moment; T is the torque; E is the Young's modulus; G is the shear modulus; I_{zz} is the moment of inertia; J_0 is the polar moment of inertia. Assuming a linearly elastic behavior, the total strain energy can be described as

$$U_{Total} = \frac{F^2(m\cos\theta)^3}{6E}\left[\frac{2(1+\nu)}{J_0} + \frac{\cos^2\theta}{I_{zz}}\right] \tag{2}$$

where ν is the Poisson's ratio; m and θ are defined in Figure 2b.

Thus, the equivalent moment of inertia (of an equivalent simply supported beam subjected to a point force) can be introduced as

$$\mathbb{I}_{eq} = \left[\frac{2(1+\nu)}{J_0} + \frac{\cos^2\theta}{I_{zz}}\right]^{-1} \tag{3}$$

It can be seen that the bending stiffness of chain-link mesh depends on the wire diameter, material's Poisson's ratio and the mesh weaving angle.

4. EXPERIMENTAL METHOD FOR DETERMINING AREA MOMENT OF INERTIA

A set of four-point bending experiments was conducted to compare the analytical predictions of bending resistance with the experimentally observed behavior. A servohydraulic uniaxial tension/compression testing machine (Instron 1350) with load capacity of 100 *kN* was used to apply the loads and measure the deflections with an integrated LVDT sensor. The loads were measured with a 1 *kN* S-beam load cell, manufactured by Futek, rigidly fixed to the testing machine. To obtain the four-point loading boundary conditions, a custom apparatus was constructed. It consisted of two frames (upper load and lower support frames) that provided a maximum support or load span of 0.75 *m*, see Figure 3.

The test procedure followed ASTM E855-90 [14]. The load applicators were centered at 2/3 of the support span distance, and the testing was conducted at two support spans: 0.75 *m* and 0.45 *m*. This was done to observe the effects due to different picket length to diamond size ratio. In addition, a series of tests were performed to study the sensitivity of the results to the setup parameters, such as picket orientation, tension in the mesh, specimen length).

Each test was repeated a minimum of six times to determine the variance in the resulting data. Prior to each set of experiments, the load cell was calibrated by zeroing it and checking it with a 100 *g* precision weight to ensure consistency. The data was recorded at the sampling frequency of 1.0 *kHz*. A crosshead velocity of 0.1 *mm*/*s* was used for all experiments.

From the sensitivity studies, the maximum displacement of all meshes in the elastic loading range was found to be 35 *mm*, resulting in a radius of curvature of 0.35 *m*. All experimental data showed significant trends of linearity. The bending resistance (*N*/*mm*) of each specimen was calculated by applying a linear regression to the measured data and calculating the slope of the curve, see Figure 4.

With the bending resistance of each specimen known, the Euler–Bernoulli linear beam theory was used to determine the picket's effective moment of inertia. The moment of inertia can be calculated using the following equation, based on a two point loaded simply supported beam [14]:

$$\delta_L = \frac{Pa}{48E\mathbb{I}_{eq}}(3L^2 - 4a^2) \tag{4}$$

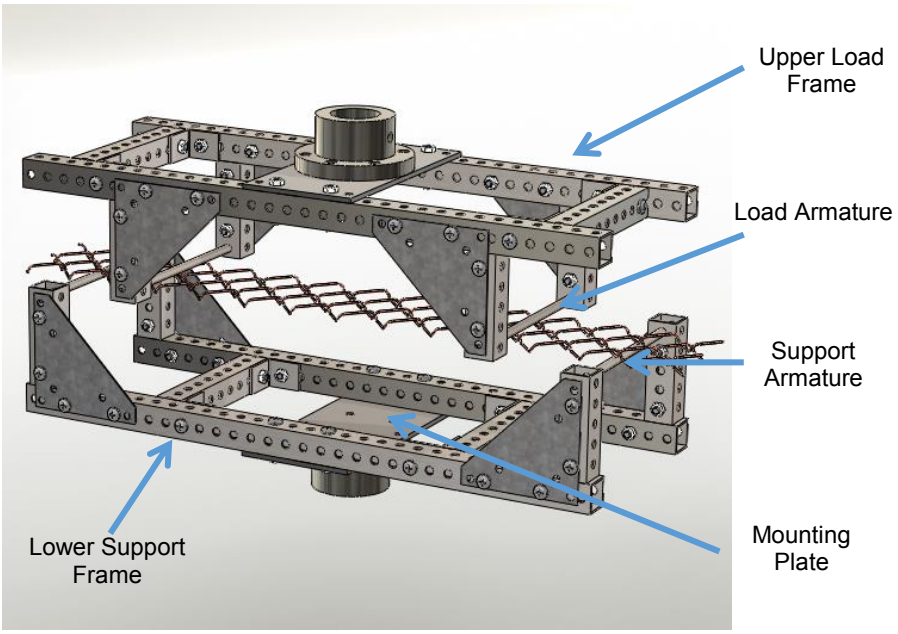

Figure 3: Schematics of the four-point bending fixture for testing of the chain-link meshes.

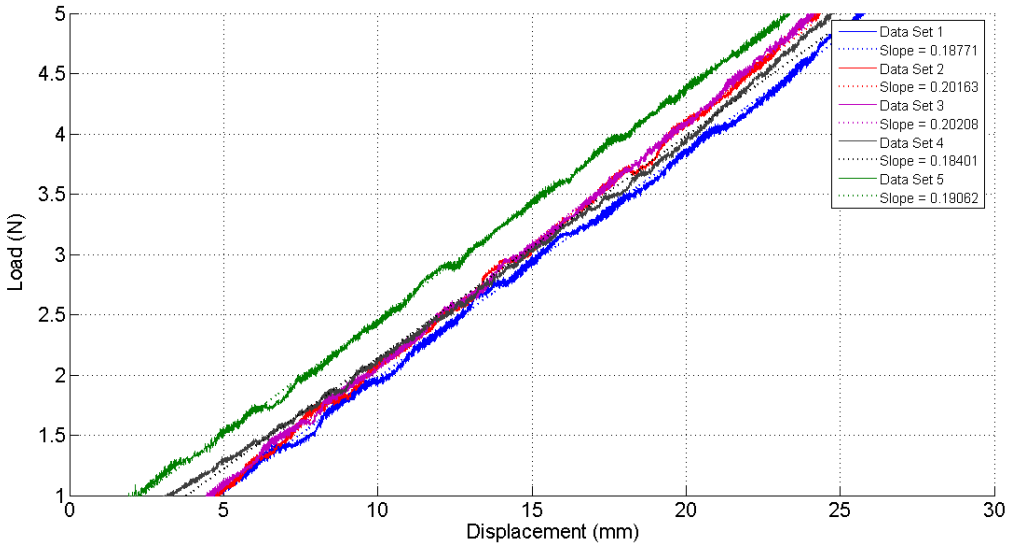

Figure 4: Example of the experimental data with linear regression slopes from a single picket bending test.

where δ_L is the deflection at the points of loading; P is the applied load; $\mathbb{I}_{eq}$ is the area moment of inertia at the origin of axes; E is the Young's modulus of the material; L is the span length between supports, and a is the distance from the support to the load point.

The results of experimental tests are presented in Table 2. It can be seen that the apparent stiffness significantly depends on the orientation of the bending plane (XY and XZ). Also, the analytical predictions and experimental values for the equivalent area moment of inertia of a single picket compare well, with a maximum relative difference lower than 17%.

It was observed that in the tests of a net panel consisting of four interconnected pickets, the observed stiffness was approximately four times higher than that of a single picket. This indicates that interaction between the pickets can be neglected in the predictions of chain-link mesh bending behavior.

Table 2: Comparison of the equivalent moments of inertia obtained from the experimental measurements and analytical predictions.

Specimen	Orientation	$\mathbb{I}_{eq}$ for 1 Picket, mm^4			$\mathbb{I}_{eq}$ for 4 Pickets, mm^4		
		Analytical	Experimental	δ^*,%	Analytical	Experimental	δ^*,%
M2.5-30	Y	1.23	1.27	3.5			
	Z	1.10	0.94	-16.8	4.39	3.82	-15.0
M2.5-25	Y	1.23	1.23	0.3			
	Z	1.10	1.04	-5.6	4.39	3.64	-20.6
Straight wire	Y	2.04	2.27	-10.4			
	Z	2.04	2.27	-10.4	8.12	9.08	-10.4
M3.5-50	Y	4.83	4.61	-4.8			
	Z	4.31	4.03	-7.0	17.3	16.8	-2.7

$$* \ \delta = \frac{\mathbb{I}_{exp} - \mathbb{I}_{ana}}{\mathbb{I}_{exp}} \cdot 100\%$$

5. NUMERICAL MODEL TO PREDICT VOLUMETRIC LOSS UNDER WAVES AND CURRENTS

A commercially sized, cylindrical gravity cage system was selected as the base framework flotation and support structure. The system has a diameter of 20 m and a net chamber depth of 10 m with a static net chamber volume of 3140 m^3. Such a system replicates a commercially sized cage presently utilized in down-east Maine fish farms. The buoyant rim is composed of two concentric floating collars constructed of 400 mm diameter HDPE pipes, and the lower rim made of a 90 mm pipe. To describe the drag forces on the net chamber, a recent study by Tsukrov et al. [13] was used. The copper alloy and nylon nets selected had a solidity of 17.1% (where solidity is the ratio of projected area to outline area). The detailed breakdown of cage framework design parameters is shown below in Table 3. The finite element mesh of the cage consisted of 1969 nodes and 2960 elements and is shown in Figure 5.

The net chamber was analyzed using both truss and beam elements to isolate the effect of the alloy's bending stiffness on the volumetric stability. For the beam elements, the effective moment of inertia was utilized as determined from the mechanical experiment.

Table 3: Cage framework model parameters.

Component parameters	Values
-FLOATATION COLLAR-	
Material	HDPE
Pipe Wall Thickness, *mm*	36
Pipe Diameter, *mm*	2x400
Collar Diameter, *m*	20
Total Mass, *kg*	5250
Young's Modulus, *GPa*	8.9
-LOWER SUPPORT COLLAR-	
Material	HDPE
Pipe Wall Thickness, *mm*	1.9
Pipe Diameter, *mm*	90
Collar Diameter, *m*	20
Young's Modulus, *GPa*	8.9
-NET CHAMBER (SIDE)-	
Twine Diameter, mm	2.54
Number of Twines per Element	35.52
-NET CHAMBER (BOTTOM)-	
Twine Diameter, mm	2.54
Number of Twines per Element	33.73

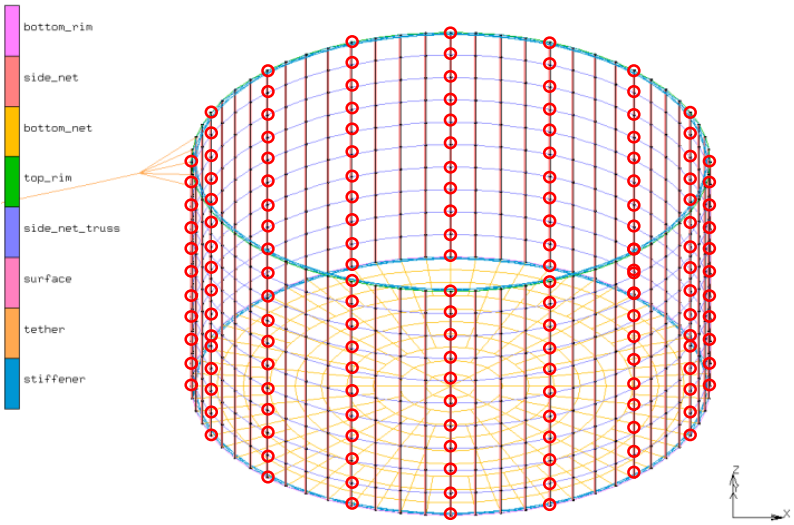

Figure 5: MSC Marc/Mentat copper-alloy cage model. Red circles indicate the tracked nodes.

Two major types of environmental loading were considered in simulations: ocean currents and waves. The wave periods and heights, and current velocities were based on the suggested off-shore aquaculture site conditions [15]. These exposed sites would experience significant wave heights between 1-3 meters (greater for storm events) with the majority of wave energy

density in the wave period range of 3 – 13 seconds [15]. To limit the number of simulations but still obtain a full range of conclusive results, a total of 11 different load cases were chosen (see Table 4). Load cases 1 through 3 (LC1-3) applied a current velocity that were constant with water depth. Load cases 4 through 7 (LC4-7) applied regular progressive waves with wave periods ranging from 5 to 11 seconds and wave heights ranging between 2 to 5 meters. Load case 8-11 (LC8-11) applied a co-linear combination of a 1 *m*/*s* current velocity with the waves.

A basic mooring system was needed to provide the vertical and horizontal freedom necessary to accurately predict the net chamber volume change. Since the applied forces are unidirectional, a simplified horizontal single point tether with length of 50 *m* was utilized.

Table 4: Simulated load cases.

Load case	Current velocity, *m*/*s*	Wave period, *s*	Wave height, m	Wave length, *m*
1	0.25	-	-	-
2	0.5	-	-	-
3	1.0	-	-	-
4	-	5	2	39
5	-	7	3	76
6	-	9	4	126
7	-	11	5	189
8	1.0	5	2	39
9	1.0	7	3	76
10	1.0	9	4	126
11	1.0	11	5	189

6. VOLUMETRIC DEFORMATION PREDICTED BY FEA

Finite element simulations were conducted to predict the volume reduction of a cage due to its deformation under waves and currents. The simulation time was set to 400 seconds with a time step of 0.0005 seconds.

Several methods are available to calculate the volume of a deformed cage based on the displacements of discrete points (nodes), for example Scalar Triple Product [3], the divergence method, and the Delaunay triangulation methods. For a detailed discussion of the volume calculation methods, see [16]. We used the divergence method and based our calculations on the data for 176 nodes evenly distributed over the net chamber, as shown in Figure 5. The volume deformation values calculated as the percentages of the remaining cage volume are shown in Table 5.

It can be seen that incorporation of the bending stiffness of netting (by using beam elements instead of truss elements) does not significantly change the predictions for the system's volume loss under the considered environmental loadings. The observed differences in volume do not exceed 3%. It appears that the ratio of beam length to resistance of bending for the analyzed system is so large that the bending stiffness of copper alloy pickets is negligible, and the netting behaves as though it was a catenary system.

Table 5: Remaining cage volume as predicted by MSC Marc simulations.

Model	Volume statistic	Load case 1	2	3	4	5	6	7	8	9	10	11
Beam elements	Mean, %	97	93	58	99	97	95	93	52	46	47	46
	Max, %				101	102	101	101	60	70	74	74
	Min, %				97	89	85	77	44	24	19	17
Truss elements	Mean, %	97	93	58	99	97	95	94	52	47	48	47
	Max, %				101	102	102	101	63	72	77	74
	Min, %				96	90	83	80	44	25	20	20

CONCLUSIONS

An experimental study was performed to characterize the bending stiffness of copper alloy chain-links meshes. The collected data was used to validate the developed analytical and numerical models. It was found that for commercial scale fish cages the bending stiffness of the copper alloy mesh does not significantly affect the predictions of volumetric loss due to environmental loading. It can be concluded that the implementation of the bending resistance of copper alloy mesh is not significant in determining the dynamic behavior of gravity type commercial fish cages. Thus, the traditional numerical modeling techniques (i.e. using truss elements) are sufficient for analyzing dynamics of copper alloy fish cage systems.

ACKNOWLEDGMENTS

The authors thank the manufacturers for supplying the test specimens. Langley Gace (International Copper Association) is acknowledged for sharing information on various copper alloy nets. The authors are grateful to Murat Yigit (Canakkale University) for providing mesh *M2.5-30* and Yannis Korkolis (University of New Hampshire) for invaluable discussions. Great thanks are extended to Paul Lavoie for help with the experiments.

REFERENCES

[1] UNFPA, "State of World Population 2011," United Nations Populations Fund, New York, NY, 2011.

[2] FAO, "Statistics and information Service of the Fisheries and Aquaculture Department," Food and Agriculture Organization of the United Nations, Rome, Italy, 2011.

[3] C.-C. Huang, H.-J. Tang and J.-Y. Liu, "Dynamical analysis of net cage structures for marine aquaculture: Numerical simulation and model testing," *Aquacultural Engineering,* vol. 35, no. 3, 2006.

[4] P. Lader, T. Dempster, A. Fredheim and O. Jensen, "Current induced net deformation in full-scale sea-cages for Atlantic salmon," *Aquacultural Engineering,* vol. 38, no. 1, pp. 52-65, 2008.

[5] Y.-P. Zhao, Y.-C. Li, G.-H. Dong, F.-K. Gui and B. Teng, "Numerical simulation of the effects of structure size ratio and mesh type on three-dimensional deformation of the fishing-net gravity cage in current," *Aquacultural Engineering,* vol. 36, no. 3, pp. 285-301, May 2007.

[6] S. Cheah and T. Chua, "A Preliminary Study of the Tropical Marine Fouling Organisms on Floating Net Cages," *Malayan Nature Journal,* pp. 39-48, 1979.

[7] R. Swift, D. W. Fredriksson, A. Unrein, B. Fullerton, O. Patursson and K. Baldwin, "Drag force acting on biofouled net panels," *Aquacultural Engineering,* vol. 35, no. 3, pp. 292-299, October 2006.

[8] J. Ortuno, M. A. Esteban and J. Meseguer, "Effects of short-term crowding stress on the gilthead seabream(Sparus aurata L.) innate immune response," *Fish Shell Immunology,* vol. 11, no. 2, pp. 187-197, 2001.

[9] R. Braithwaite, M. C. C. Carrascosa and L. McEvoy, "Biofouling of salmon cage netting and the efficacy of a typical copper-based antifoulant," *Aquaculture,* vol. 262, no. 2-4, pp. 219-226, 28 February 2007.

[10] A. Drach, I. Tsukrov, T. Gross, U. Hofmann, J. Aufrecht and A. Grohbauer, "Corrosion rates and changes in mechanical properties of copper alloys due to seawater exposure, IMECE2012-88156," in *Proceedings of the ASME 2012 International Mechanical Engineering Congress & Exposition*, Houston, TX, USA, 2012.

[11] H. Moe, R. H. Gaarder, A. Olsen and O. S. Hopperstad, "Resistance of aquaculture net cage materials to biting by Atlantic Cod (Gadus morhua)," *Aquacultural Engineering,* vol. 40, no. 3, pp. 126-134, May 2009.

[12] A. Drach, I. Tsukrov, J. DeCew, U. Hofmann, J. Aufrecht and A. Grohbauer, "Corrosion and biofouling performance of copper alloys investigated in the North Atlantic Ocean," in *CORROSION/2013*, Houston, TX, USA, 2013.

[13] I. Tsukrov, A. Drach, J. Decew, M. R. Swift and B. Celikkol, "Characterization of geometry and normal drag coefficients of copper nets," *Ocean Engineering,* vol. 38, no. 17-18, pp. 1979-1988, September 2011.

[14] ASTM E855-08, "Standard test methods for bend testing of metallic flat materials for spring applications involving static loading," ASTM International, West Conshohocken, PA, 2009.

[15] J. Ryan, "Farming the Deep Blue," Westport, Ireland, 2004.

[16] M. Osienski, "Dynamic and structural analyses of a gravity fish cage employing copper alloy netting," University of New Hampshire, Durham, NH, 2013.